Protein Cell 2011, 2(10): 814–826
DOI 10.1007/s13238-011-1090-6

Protein & Cell

RESEARCH ARTICLE

Crystal structure of human Gadd45 reveals an active dimer

Wenzheng Zhang[1,2,3*], Sheng Fu[1*], Xuefeng Liu[4], Xuelian Zhao[4], Wenchi Zhang[1], Wei Peng[1], Congying Wu[3], Yuanyuan Li[3], Xuemei Li[1], Mark Bartlam[1,2], Zong-Hao Zeng[1] ✉, Qimin Zhan[4] ✉, Zihe Rao[1,2,3]

[1] National Laboratory of Biomacromolecules, Institute of Biophysics, Chinese Academy of Sciences, Beijing 100101, China
[2] Tianjin Key Laboratory of Protein Science, College of Life Sciences, Nankai University, Tianjin 300071, China
[3] Laboratory of Structural Biology, Tsinghua University, Beijing 100084, China
[4] State Key Laboratory of Molecular Oncology, Cancer Institute, Chinese Academy of Medical Sciences and Peking Union Medical College, Beijing 100021, China
✉ Correspondence: zzh@ibp.ac.cn (Z.-H. Zeng), zhanqimin@pumc.edu.cn (Q. Zhan)
Received August 23, 2011 Accepted September 19, 2011

ABSTRACT

The human Gadd45 protein family plays critical roles in DNA repair, negative growth control, genomic stability, cell cycle checkpoints and apoptosis. Here we report the crystal structure of human Gadd45, revealing a unique dimer formed via a bundle of four parallel helices, involving the most conserved residues among the Gadd45 isoforms. Mutational analysis of human Gadd45 identified a conserved, highly acidic patch in the central region of the dimer for interaction with the proliferating cell nuclear antigen (PCNA), p21 and cdc2, suggesting that the parallel dimer is the active form for the interaction. Cellular assays indicate that: (1) dimerization of Gadd45 is necessary for apoptosis as well as growth inhibition, and that cell growth inhibition is caused by both cell cycle arrest and apoptosis; (2) a conserved and highly acidic patch on the dimer surface, including the important residues Glu87 and Asp89, is a putative interface for binding proteins related to the cell cycle, DNA repair and apoptosis. These results reveal the mechanism of self-association by Gadd45 proteins and the importance of this self-association for their biological function.

KEYWORDS crystal structure, Gadd45, dimer, DNA repair, growth inhibition, apoptosis

INTRODUCTION

The human Gadd45 family of growth arrest and DNA damage-inducible proteins has three members, Gadd45α, -β, and -γ, grouped together on the basis of their amino acid sequences and functional similarities (Vairapandi et al., 1996; Takekawa and Saito, 1998; Nakayama et al., 1999). The genes encoding the α, β and γ isoforms of Gadd45 are respectively located at 1p31.2, 19p13.3 and 9q22.1 in the human genome, and they have different promoters and introns (Kastan et al., 1992; Jung et al., 2000; Lefort et al., 2001; Furukawa-Hibi et al., 2002; Thyss et al., 2005). Each gene is induced by a distinct subset of environmental and physiological stresses (Liebermann and Hoffman, 2007). The three Gadd45 proteins are small (18 kDa), highly acidic and evolutionarily conserved. The amino acid sequence identities among the three members are 51%–56%, either in human or in mice, while the identities between the human proteins and their mouse counterparts are 93%–95%.

The Gadd45 proteins can interact directly with a wide variety of proteins, including cdc2/cdk1, and the cdc2/Cyclin B1 complex (Zhan et al., 1999; Jin et al., 2000; Vairapandi et al., 2002). Interestingly, Gadd45α and Gadd45β, but not Gadd45γ, can disrupt the cdc2/Cyclin B1 complex (Vairapandi et al., 2002). The Gadd45 proteins also interact with the proliferating cell nuclear antigen, PCNA (Vairapandi et al., 2000; Azam et al., 2001); the cyclin-dependent kinase

[*] These authors contributed equally to the work

inhibitor $p21^{WAF1/Cip1}$ (Kearsey et al., 1995; Zhao et al., 2000); MEKK4/MTK1 (Takekawa and Saito, 1998); MKK7/JNKK2 (Papa et al., 2004); p38 (Bulavin et al., 2003); the cell death repressor Bcl-xL and the anti-apoptotic domain of cytomegalovirus vMIA (Smith and Mocarski, 2005); nuclear hormone receptors (Jung et al., 2000); histone (Carrier et al., 1999); the transcription factor CRIF1/Gadd45GIP1 (Chung et al., 2003); the Aurora-A protein kinase (Shao et al., 2006) which is implicated in the centrosome cycle; the nucleophosmin (also termed B23) (Gao et al., 2005); and the DNA repair endonuclease XPG (Barreto et al., 2007).

The Gadd45 proteins are able to form homo- or hetero-oligomers with other family members via hydrophobic interactions (Kovalsky et al., 2001). Numerous experiments have shown that the Gadd45 proteins can play important roles in many critical biological processes and directly interact with a diverse range of molecules, yet their precise roles and biological functions remain unclear. In order to further illuminate the roles and functions of the Gadd45 proteins, we have determined and analysed the crystal structure of human Gadd45γ. The crystal structure of an N-terminal truncated mouse Gadd45γ was recently reported (Schrag et al., 2008). Moreover, another crystal structure of Gadd45γ has been deposited into the Protein Data Bank (PDB) with code 2WAL, enabling us to compare and discuss the mode of dimerization observed in the three crystal structures. Furthermore, mutational analysis and cellular assays of human Gadd45γ shed light on the relationship between the structure and biological function of Gadd45 proteins.

Authors from the Cancer Institute are working on cell biology. Dr. Qimin Zhan, one of the corresponding authors, has been working with Gadd45 proteins for years and published more than 50 papers related to the function of Gadd45 proteins.

RESULTS AND DISCUSSION

The monomer structure of human Gadd45

The crystal structure of human Gadd45γ, with additional 8 residues at the N-terminal, was determined to 2.3 Å with a final R-factor of 23.3% and free R-factor of 26.6% (Table S1). The structure has one molecule per asymmetric unit in space group $I2_13$ (Fig. S1). There are no experimental electron densities for the N-terminal 14 + 8 residues.The structure model contains the remaining residues, from 15 to 159, folding into a compact structure, containing five-strand β sheet, surrounded by five α helices (Fig. 1). The α helices and β strands are alternately arranged throughout the sequence. There are also three loops, L1, L2 and L3, in between of B2 and H3, H4 and B4, and B4 and H5, respectively. Except L1, loops L2 and L3 are disordered, and therefore, poorly defined.

The five β-strands compose a β-sheet, from left to right, and they are arranged as B1-B4-B2-B3-B5. The left three strands, B1-B4-B2, are anti-parallel, while the right three, B2-B3-B5, are parallel. Below the β-sheet are three helices, H1, H4 and H5, two of which (H1 and H5) are perpendicular to the β-strands. Above the β-sheet, the helices H2 and H3 are parallel with each other and approximately parallel (or antiparallel) with the β-strands. The five-strand β-sheet and the helices H2, H3 and H5 are the most stable part of the protein, as shown by the crystallographic B factors (Fig. S2). The interaction between the side chains of Asp68 and His118 makes the acidic loop, L1, connecting B2 and H3 less flexible as one might expect from its amino acid sequence, AGEEDEGD. Protruding out from the molecule, the two helices, H2 and H3, are packed against the β sheet. A number of hydrophobic residues are distributed on these two helices, making up a hydrophobic area on the molecular surface. This provides a surface pacth for dimer formation.

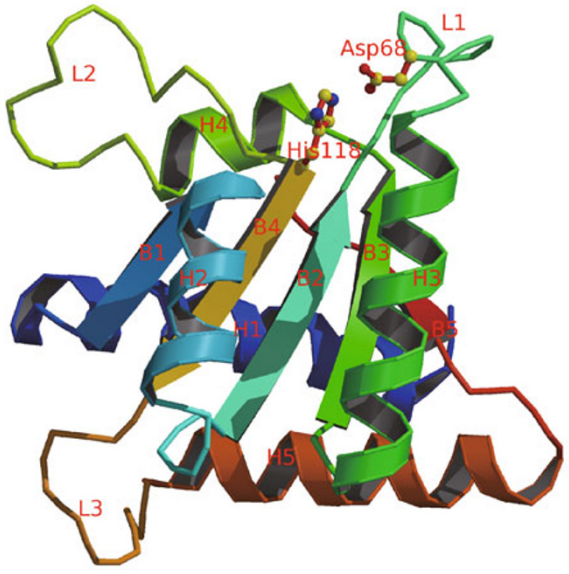

Figure 1. The structure of human Gadd45. The sequence folds into five α helices and five β strands, including three loops, sequentially arranged as H1-B1-H2-B2-L1-H3-B3-H4-L2-B4-L3-H5-B5. The five β strands spacially arranged as a β sheet, B1-B4-B2-B3-B5, surounded by the helices. Figures 1–4 are created using Molscript (Kraulis, 1991) and Raster3D (Merritt and Bacon, 1997).

The human Gadd45γ dimer structures

In the crystal, each monomer is directly in contact with five others (Fig. S3). Among these monomer-monomer interfaces, only one has a significant buried monomer surface area of 1585 $Å^2$, while the next largest has only 541 $Å^2$, not comparable with the largest one.

The largest interface leads to a dimer, consisting of two monomers related by a crystallographic 2-fold axis (Fig. 2). At

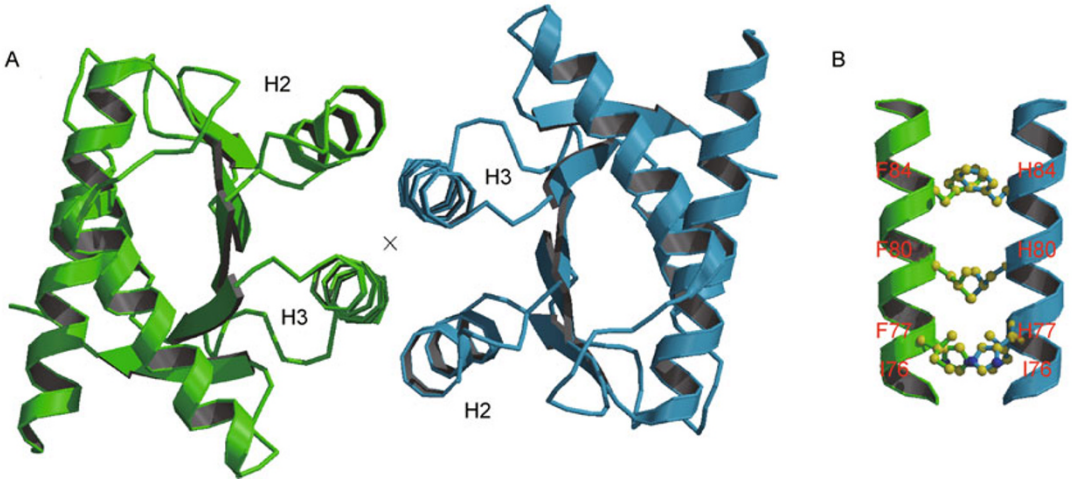

Figure 2. The human Gadd45γ dimer structures. The 2-fold crystallographic axis relating the two monomers is nearly parallel to H3 and is just at the middle point of the two H3's (the cross in A). Therefore, the dimer is formed by parallell packing of the four α helices, two H2's and two H3's. (A) The view along the 2-fold axis; (B) The side view of the packing of the two H3's.

the interface, the four α helices, two H2's and two H3's, are parallell and interleaved. Interactions mainly occur between the H3 from one monomer with H2 and H3 from another. The ridge of each H3 penetrates into the cavity between H2 and H3 of the neighboring monomer. The side chain of Leu80 on H3 reaches the bottom of the cavity, with distances between Leu80:Cδ2 and Ile81:Cδ of 3.3 Å, and between Leu80:Cδ2 and Ala47:Cβ of 3.6 Å, respectively (Fig. 3).

The part of the monomer surface provided by H2 and H3 is hydrophobic, as measured by buried surface areas. In the 1585 $Å^2$ areas, 1192 $Å^2$ is hydrophobic (provided by C atoms) and 393 $Å^2$ is hydrophilic (provided by N, or O atoms). This is in agreement with the report by Kovalsky et al. (2001). In fact , the distribution of crystallographic B factors (Fig. S2) shows that the dimer interface and the neighbouring regions, as a hydrophobic core, is the most stable part of the dimer.

Comparison with the mouse Gadd45γ structure

The two amino acid sequences of human and mouse Gadd45γ are very similar, and among the 159 residues only 7 are in difference. Therefore they should also have similar three dimensional structures. In fact, one gets a root mean square deviation of 1.1 Å for all 127 Cα atoms appearing in the three models, two from the mouse Gadd45γ structure (Schrag et al., 2008). A significant difference is the shift of helix H2 away from H3 in the human Gadd45γ structure. The Ala47:Cα (on H2) to Ile81:Cα (on H3) distance is increased from 6.4 Å in the mouse structure to 8.1 Å in the human structure. The most likely reason for this structural change is to enable the side chain of Leu80 (on H3) from the neighboring monomer to embed itself inside (Fig. 3).

At the dimer level, the mouse dimer (the one proposed by Schrag et al. based on the mouse crystal structure) also uses

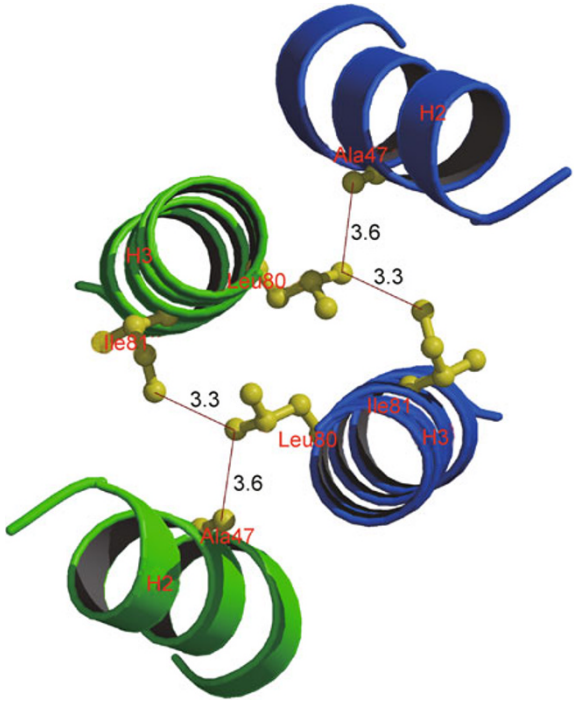

Figure 3. Close packing of the four helices in human Gadd45γ dimer. Helices of the two monomers are colored, in green and blue, respectively. Numbers and red lines indicating the atomic distances in unit of Å. The interleaved packing of the four helices lets the H3 reach the sunken surface in between of H2 and H3 on the opposite monomer. One may notice that in a monomer, the residue Ile81 on H3 directs to H2 and B2 (not shown), not quite a surface residue.

H2 and H3 for dimer forming, but in an antiparallell and ridge-to-ridge manner (Fig. 4). Furthermore, there is a relative shift,

Figure 4. Packing of the antiparallell dimer identified by Schrag et al. (A) The four helices are packed in a ridge-to-ridge manner. Hollow spaces that allow solvents exsit in between the four helices. (B) Packing of the two H3 helices. Only part of the helices takes part in interaction.

by about two-fifths of the helix length, of the two H3's relative to each other. The buried surface area is 917 Å^2 (735 Å^2 hydrophobic and 182 Å^2 hydrophilic), much smaller than the parallel interface, and even much smaller than the one also existing in the mouse crystal but ignored by Schraf et al.. The parallel interface is compact and has a deeply buried hydrophobic core (Fig. 2), while the anti-parallel interface is narrowed by the holes and all the residues on the interface are still solvent accessible (Fig. 4).

At the very beginning, the identification of the antiparallell dimer is somewhat questionable. Tetramers exist in the mouse crystal and there are two ways to split the tetramer into dimers. Try to support their selection of the antiparallel dimer, Schrag et al. performed mutation at site 80, but this site is at the center of the tetramer, taking part in both types of interfaces. There are no experimental, as well as theoretical, evidence to ignore the much larger interface and identify the much smallar one (Schrag et al., 2008).

Effects of mutations on dimerization

To further define the properties of the dimer interface and understand the mechanism of dimerization, mutations were introduced into various sites in the interface to replace hydrophobic residues with hydrophilic ones (Fig. S4). Results indicate that multiple-site mutations commonly disrupt the dimer more strongly than any single mutation. In general, apparent molecular weights (MW) determined according to the corresponding calibration curve (data not shown) are mostly greater than the monomer mass, but less or equal to the dimer mass (Table S2). Dynamic light scattering also reveals similar behaviors (Fig. S5D), indicating that the apparent masses are weighted means of monomers and dimers. Multiple-site mutants generally have lower apparent masses and therefore higher dissociation constants. Mutation of amino acids on both H2 and H3 helices tends to be more effective on disrupting the dimer than mutations on only one helix, H3 (compare apparent MW of A47R + F84R with those of I76E + L80E + A83R and I76R + H77R + L80R, the sites for mutation are shown in Fig. S4) .

To gain a more quantitative measure of the interactions involved in dimerization, analytical ultracentrifugation (AUC) experiments (Fig. S5E and S5F) on both wild-type and mutant proteins were performed and give the dissociation constant, k_d, of dimerization as 0.5 ± 0.22 μmol/L for the wild type and 17.88 ± 6.04 μmol/L for the A47R + I76E + L80E + A83R mutant. The dissociation constant of wild-type Gadd45γ lies between the reported k_d values for Gadd45α (0.4 μmol/L) and Gadd45β (10 μmol/L) (Kovalsky et al., 2001; Tornatore et al., 2008).

The above data from mutational analysis demonstrates that the surfaces of H2 and H3 are the most likely dimer-forming surface, but is not sufficient to distinguish between parallel and anti-parallel packing. The dimerization interfaces from different crystal packing therefore require verification by other means. In fact, the structure of the parallel dimer is strikingly dissimilar from that of anti-parallel dimer (Fig. 5C and 5D), suggesting different functional consequences. Thus, a series of functional assays were performed to test the validity of the parallel dimer for various functions of Gadd45γ.

Colony formation assay

Based on the crystal structure of human Gadd45γ dimer, we were interested in whether or not the dimer was a definitive factor in growth inhibition. We therefore employed a colony formation assay in HeLa and EC9706 cell lines to investigate the influence of dissociation of the human Gadd45γ dimer on growth inhibition. The E87K + D89K mutant, verified to be dimeric from our experiments (Fig. S5A2 and S5D), was also

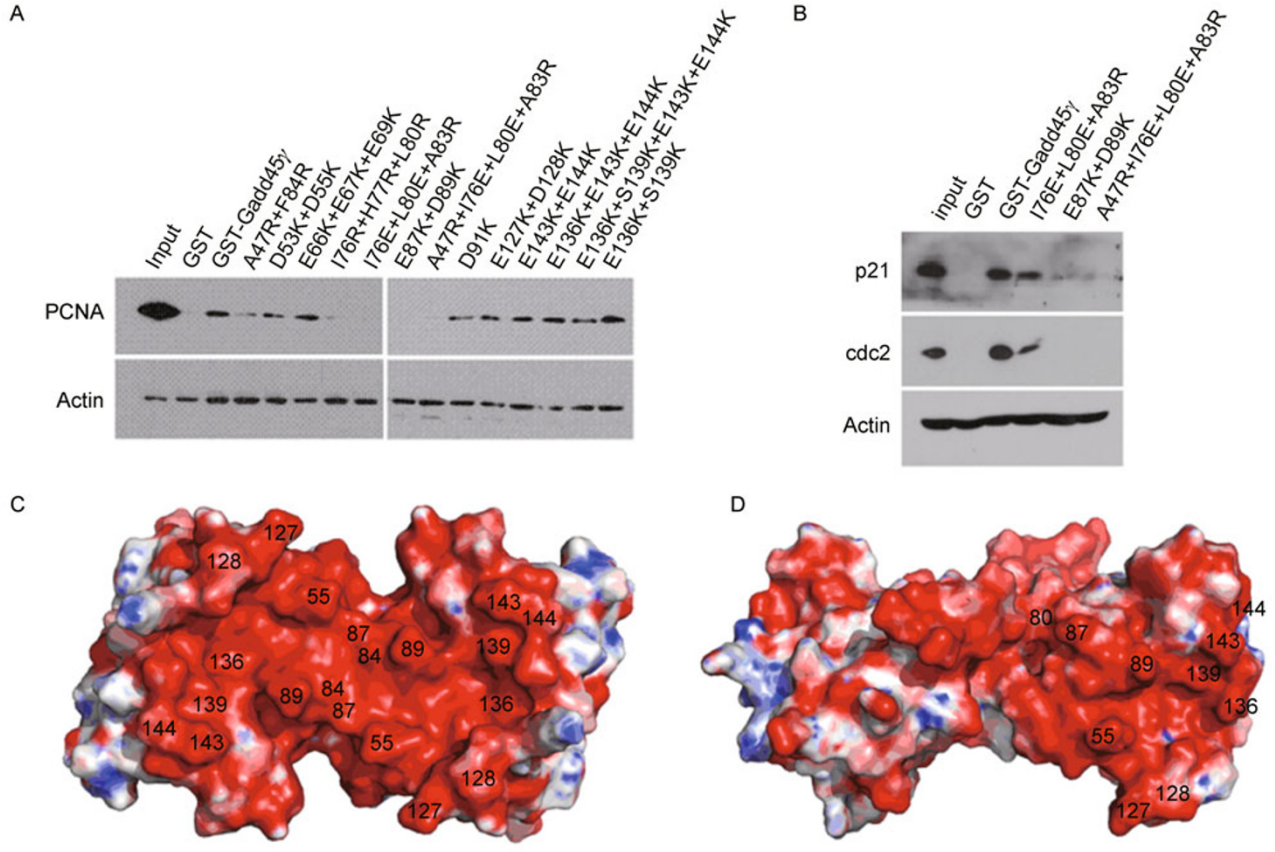

Figure 5. Binding of human Gadd45γ and its mutants to PCNA (A) or p21 and cdc2 (B). HeLa cell lysates were incubated with human Gadd45γ and its mutants, and a pull-down assay was performed to detect interactions with PCNA, p21 or cdc2. Actin levels in 10 μL total material were used as input control. (C) The putative PCNA-binding region on the bottom of the full-length human Gadd45γ dimer. (D) The equivalent region of the truncated mouse Gadd45γ dimer, shown in a similar orientation as C. Fig. 5C and 5D are drawn with PyMol (www.pymol.org).

selected to test its growth inhibition ability. Figure 6 shows that similar results were obtained from both cell lines. The two dimer-dissociating mutants, I76E + L80E + A83R and A47R + I76E + L80E + A83R, greatly decreased the ability of growth inhibition compared to wild-type Gadd45γ (~90%). Furthermore, the A47R + I76E + L80E + A83R mutant which has a stronger capability of dissociating the dimer showed a weaker inhibitory effect on cell growth (~20%), strongly suggesting that dimerization of Gadd45γ is essential for growth inhibition. Notably, the E87K + D89K mutant also inhibited cell growth but more weakly than the wild-type Gadd45γ, retaining only about 51% and 78% of the growth inhibition in HeLa and EC9706 cells respectively. This observation implies that dimerization alone cannot account for growth inhibition and suggests that mutations at these two sites may reduce the growth inhibition ability of the dimer by affecting the binding of Gadd45γ to partners that can induce growth suppression. However, the E87K + D89K mutant does exhibit some cell line dependent effects.

Analysis of the cell cycle distribution

Gadd45γ can induce or may regulate cell cycle arrest at the G_1 or G_2/M phase via its interaction with p21 and cdc2 or cdc2/Cyclin B1 (Kearsey et al., 1995; Zhan et al., 1999). We thus set out to determine whether the inability of dimer-dissociating mutants of Gadd45γ to inhibit growth is related to an inability to induce cell cycle arrest. The wild-type Gadd45γ group showed a significantly increased percentage of cells in the G_1 phase in HeLa cell lines compared to the control group ($p < 0.05$) (Fig. 7). In contrast, the I76E + L80E + A83R and A47R + I76E + L80E + A83R mutants did not arrest cell cycle at the G_1 phase, particularly the A47R + I76E + L80E + A83R mutant ($p > 0.05$). Furthermore, there is a significant difference between the wild type and a mutant A47R + I76E + L80E + A83R ($p < 0.05$), but not between the wild type and mutant I76E + L80E + A83R ($p > 0.05$). These results indicate that the loss of cell growth inhibition by the dimer-dissociating mutants of Gadd45γ might be associated with the loss of cell

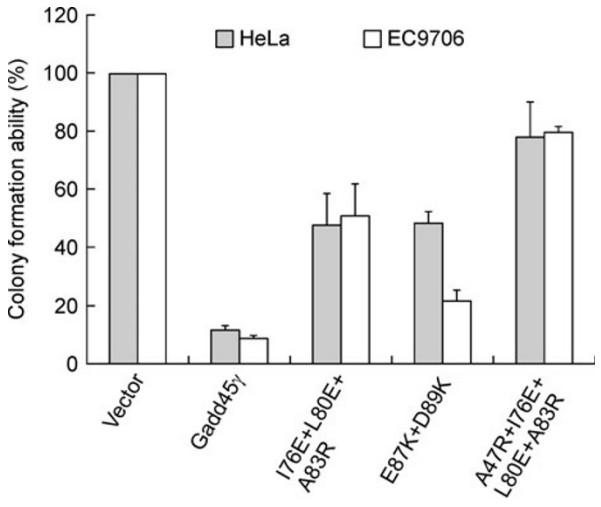

Figure 6. Colony formation efficiency of human Gadd45γ and its mutants in HeLa and EC9706 cells. Transfected cells were selected with G418 for 2–3 weeks, and the surviving colonies were counted after staining with 0.5% crystal violet. The numbers of G418 resistant colonies in control vector transfected cells were set to 100%. Columns show the mean of three separate experiments; bars show the SD.

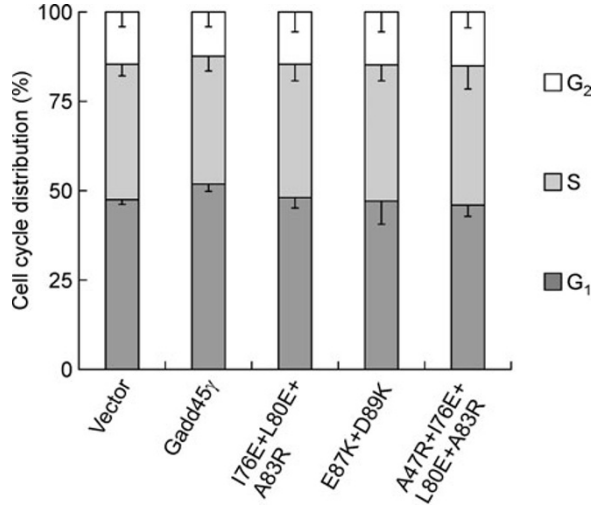

Figure 7. Cell cycle profile of human Gadd45γ and its mutants in HeLa cells. Cells were transfected with the indicated pcDNA3.1(+) vectors. Cell cycle distribution of Gadd45γ, mutant forms, and the empty control vector were measured by propidium iodide (PI) staining followed by flow cytometry after transfection for 48 h. Results are the mean ± SD from triplicate experiments.

cycle arrest at the G_1 phase. In other words, the dimerization of Gadd45γ should facilitate to induce cell cycle arrest at the G_1 phase. Moreover, the cell cycle distribution of the E87K + D89K mutant group exhibited no significant differences from the control group, suggesting that these two residues are also involved in the control of cell cycle progression.

Measurement of apoptosis

Expression of Gadd45γ has been shown to induce cell apoptosis in mammalian cell lines (Takekawa and Saito, 1998), prompting us to ask whether the dimerization was also a major factor for apoptosis. We therefore performed apoptosis assays using DAPI staining in HeLa cells following exposure to both low and high doses of UV irradiation (Fig. 8). As expected, wild-type Gadd45γ exhibited the highest apoptotic rate in both low and high doses of UV irradiation (28% and 54%, respectively). However, the I76E + L80E + A83R and A47R + I76E + L80E + A83R mutants exhibited a significant decrease in their ability to induce apoptosis, particularly the A47R + I76E + L80E + A83R mutant, which almost entirely lost its ability to induce apoptosis (8.5% and 22%, respectively) with similar levels to the empty vector group (5% and 12%, respectively). These results indicate that dimerization of Gadd45γ is necessary for inducing apoptosis and the inability of dimer-dissociating mutants of Gadd45γ to inhibit growth is also related to an inability of inducing apoptosis. The dimeric E87K + D89K mutant also exhibited a decreased ability to induce apoptosis (18% and 35%, respectively), which may be due to a weakened interaction of the mutant dimer with other apoptosis proteins. The molecular basis for this phenomenon remains to be elucidated.

Furthermore, as the triple and particularly the quadruple dimer-dissociating mutants gave rise to a greatly reduced apoptotic rate, this result implies that dimerization is likely to be more important for inducing apoptosis than residues Glu87 and Asp89.

Interaction between human Gadd45γ and PCNA

To gain insight into the biological function of the Gadd45γ-PCNA interaction, a pull-down approach was employed to identify specific sites that mediate the interaction of Gadd45γ with PCNA. Positive signals for PCNA were detected for the GST-Gadd45γ pull-down-complex with both wild-type Gadd45γ and most mutants. PCNA was not found or weak signals were detected in the pull-down complex with A47R + F84R, I76R + H77R + L80R, I76E + L80E + A83R, E87K + D89K and A47R + I76E + L80E + A83R mutants (Fig. 5A). Mutations on the acidic loop L1 (E66K + E67K + E69K) did not affect PCNA binding. These results suggest that: (1) dimers bind to PCNA more effectively than monomers; and (2) the central symmetrical region on the bottom surface of the dimer, including residues Glu87 and Asp89 from both monomers, is the putative PCNA-binding surface (Fig. 5C). Mutation of residues surrounding this region, including 55, 127, 128, 136, 139, 143 and 144, did not affect PCNA binding, and so our

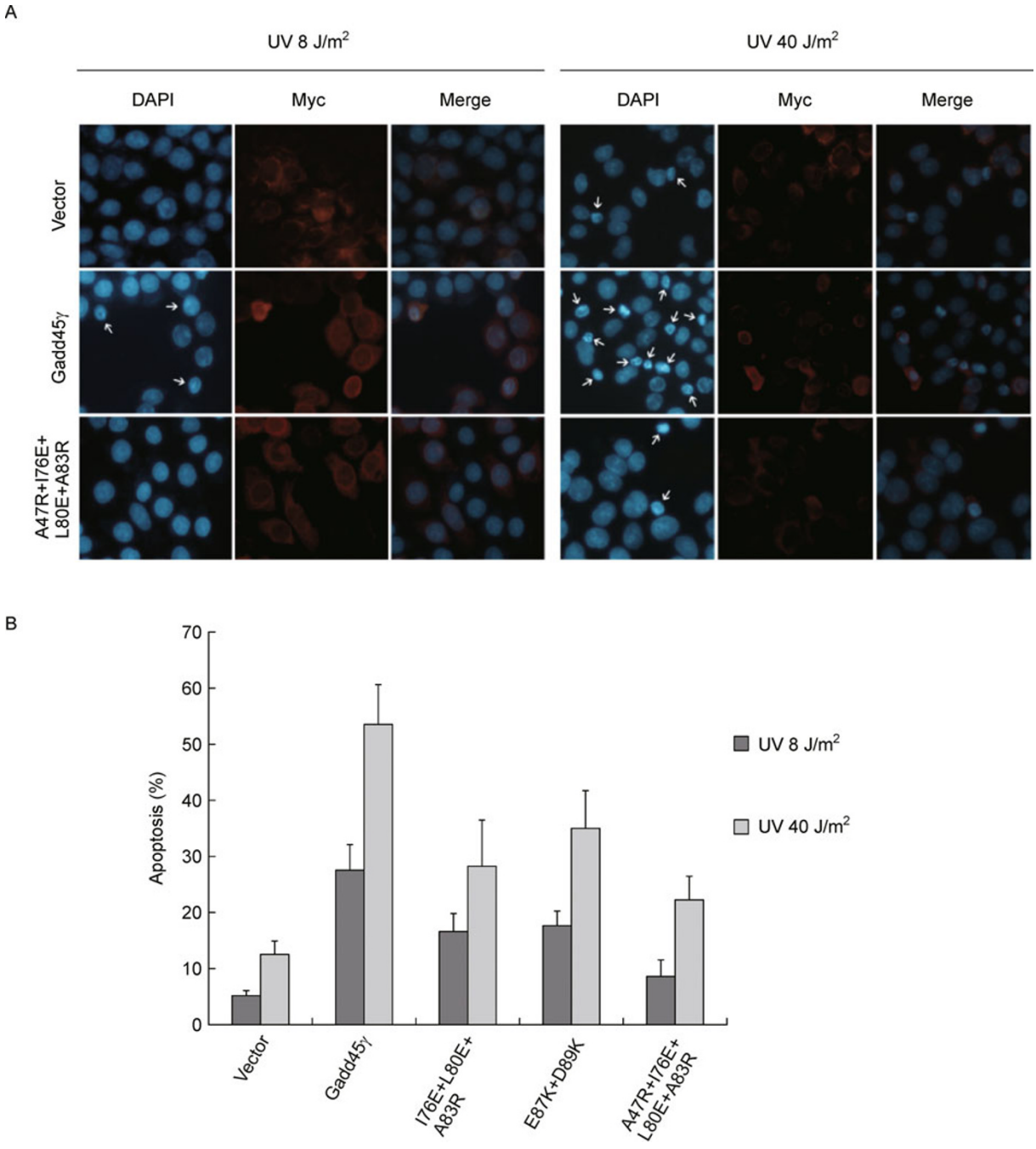

Figure 8. Effects of human Gadd45γ and its mutants on both low and high doses of UV-induced apoptosis in HeLa cells. (A) Typical cytograms for empty control vector, Gadd45γ, and A47R + I76E + L80E + A83R mutant are presented. Nuclear DNA was stained with DAPI. The transfected cells were monitored by the expression of Myc or Myc-fusion protein as stained in red. The Myc-positive apoptotic cells were indicated by arrowheads. (B) Quantitive analysis of apoptosis. Apoptotic rates were determined by dividing the number of Myc-positive cells that exhibit apoptotic morphology by the total number of Myc-positive cells. At least 400 cells from six randomly chosen fields were counted for each data point. Data are represented as mean ± SD.

results should delineate the central PCNA-binding surface. This region formed by the two symmetry-related monomers is the most negatively charged portion of the dimer surface and is most conserved among the three Gadd45 isoforms, with only Glu87 in Gadd45γ substituted by Asp84 in Gadd45β. Formation of the PCNA-binding region on the dimers via a parallel four-helix bundle consisting of two H2 helices and two H3 helices would explain why each of the Gadd45 proteins can bind to PCNA (Fig. 5C). In contrast, the "anti-parallel" dimer does not possess equivalent negative charge on its surface (Fig. 5D).

Interaction of Gadd45γ and its mutants with p21 and cdc2

Gadd45 proteins can directly interact with p21 and cdc2 or cdc2/Cyclin B1 to induce or may regulate cell cycle arrest (Kearsey et al., 1995; Zhan et al., 1999). Therefore, the inactivation of dimer-dissociating mutants of Gadd45γ on cell cycle arrest might be associated with the loss of the interaction with these proteins. As shown in Fig. 5B, glutathione S transferase (GST)-pull down results demonstrate that the human wild-type Gadd45γ has positive signals for both p21 and cdc2, while the mutant I76E + L80E + A83R shows weaker binding ability compared with the wild-type. Moreover, the mutant A47R + I76E + L80E + A83R, which can almost fully dissociate the dimer, has little or no interaction with p21 or cdc2. The quadruple mutant dissociates the dimer more effectively than the triple mutant and has lesser interaction with p21 or cdc2, and thus these results indicate that dimerization is required for interaction with p21 and cdc2 and the binding activity is inversely related to the ability to dissociate dimers. Considering the known mechanisms (Kearsey et al., 1995; Zhan et al., 1999), the inability of the quadruple mutant to bind p21 and cdc2 is consistent with its inability to cause cell cycle arrest at the G_1 or G_2 phase in HeLa cell lines. The dimeric E87K + D89K mutant also does not or faintly interact with p21 and cdc2, implying that the two residues are involved in the interaction. This also explains why the E87K + D89K mutant cannot arrest the cell cycle at G_1 or G_2 phase. These results strongly suggest that dimerization facilitates interaction with p21 and cdc2, and that Glu87 and Asp89 constitute very important residues for interaction with these two proteins.

The parallel dimer provides a putative binding region for recognition of various partners

In unstressed cells, the expression level of Gadd45 proteins is very low, with Western blot analysis indicating only a few femtomoles of Gadd45 per 10^6 cells (Carrier et al., 1999), and with the concentration of Gadd45γ well below the dissociation value k_d. The Gadd45 molecules in unstressed cells are expected to be monomer with unknown functions. Under environmental stresses such as ultraviolet radiation or harmful chemicals, however, Gadd45 proteins would be recruited in higher concentrations, leading to dimerization. The Gadd45 dimers would then bind to cdc2 or cdc2/Cyclin B1, inhibiting its kinase activity or dissociating the G_2/M transition complex cdc2/Cyclin B1, resulting in G_2/M arrest (Wang et al., 1999; Zhan et al., 1999; Jin et al., 2002; Vairapandi et al., 2002; Sun et al., 2003; Mak and Kültz, 2004). Similarly, Gadd45 dimers also can bind to p21, and may modulate or synergistically facilitate G_1/S arrest (Kearsey et al., 1995; Zhan et al., 1999; Zhao et al., 2000). Alternatively, Gadd45 dimers would interact with PCNA to aid in nucleotide excision repair of DNA (Smith et al., 2000).

Other groups reported that the effects of wild-type and mutants of Gadd45γ on cell growth parallel their abilities to dimerize, indicating that dimerization is essential for growth inhibition (Schrag et al., 2008). Similar outcomes were observed in HeLa and EC9706 cells, and we drew the same conclusion. In addition, the results of cellular assays and GST pull-down assays for the E87K + D89K mutant indicate that it also reduces the growth inhibition ability of Gadd45γ (Fig. 6), which is consistent with this mutant's inability in cell cycle arrest (Fig. 7) and apoptosis (Fig. 8), and strongly suggest the binding with residues Glu87 and Asp89 to partners that can induce growth suppression or apoptosis is another crucial factor for growth inhibition or apoptosis besides the dimerization. Gadd45 proteins can block either G_1/S or G_2/M transitions (Fan et al., 1999), or stimulate DNA excision repair *in vitro* and inhibit entry of cells into S phase (Smith et al., 1994). Furthermore, ectopic expression of Gadd45α, Gadd45β, or Gadd45γ in both H1299 and M1 cells, in the absence of genotoxic stress, retards cell growth and increases the accumulation of cells in the G_1 phase of the cell cycle (Harkin et al., 1999). Our findings exhibit similar results (Fig. 7), leading us to believe that interaction of Gadd45 proteins with p21 plays a pivotal role in G_1 cell cycle arrest. The p21-binding domain of Gadd45 also encodes the cdc2-binding activity, indicating that the central region of Gadd45 may serve as an important "core" through which Gadd45 proteins can "cross-talk" with other cell cycle regulators (Zhao et al., 2000). Effects of the E87K + D89K mutant in colony formation assays (Fig. 6), cell cycle analysis (Fig. 7) and apoptosis assays (Fig. 8) suggest mutation of these two sites should affect the binding of Gadd45γ to other molecules which induce growth inhibition or apoptosis, such as p21, cdc2/cdk1 or cdc2/Cyclin B1. Our GST pull-down assays (Fig. 5A and 5B) and above analysis support the most conserved, acidic region of the Gadd45γ dimer, including residues Glu87 and Asp89 from both monomers (Fig. 5C), as being in or near the above "core," and indicate that it is the common binding region for many partners of Gadd45 proteins, such as PCNA, p21 and cdc2/cdk1. Our results, both *in vitro* and *in vivo*, point towards the parallel Gadd45γ dimer as a functional dimer, and suggest the highly conserved

acidic region (Fig. 5C) on the parallel dimer surface provides an interface for recognition and interaction with various binding partners.

CONCLUSIONS

Our results support the proposition that the parallel human Gadd45γ dimer is an active form for interaction with PCNA, p21 and cdc2. A central conserved, acidic patch on the surface of the parallel dimer was identified as the putative region that binds PCNA, p21 and cdc2 (Fig. 5C). Conservation of this binding region suggests that all Gadd45 homo- and hetero-dimers of the Gadd45 family can bind PCNA, p21 and cdc2. Cellular assays demonstrate the dimerization of Gadd45γ is essential for growth inhibition and cell growth inhibition of Gadd45γ might be associated with the cell cycle arrest at G_1 phase and apoptosis. Dimerization of Gadd45γ is also shown to be necessary for induction of apoptosis. The molecular mechanism by which cells undergo Gadd45-mediated growth inhibition and DNA repair or apoptosis following various environmental stresses can be explained by dimerization of Gadd45 proteins and their relevant interaction with molecules related to the cell cycle, DNA repair and apoptosis.

Gadd45γ has a number of different effects in the cell, and the existence of different modes of dimerization is possible. Different dimerization modes might lead to different dimer surfaces, therefore promoting different processes in the cell. More work is needed to identify diverse biological significances resulting from different modes of dimerization, and to illuminate the molecular mechanisms for the diverse effects in the cell.

MATERIALS AND METHODS

Gene cloning and protein expression

A cDNA fragment (Gadd45γ) encoding human Gadd45γ was cloned into the GST-tagged expression plasmid pGEX-6P-1 vector (Amersham Biosciences) using the *Eco*R I and *Xho* I restriction sites. Comparing the sequence of our construct with the originally submitted sequence of human Gadd45γ (GenBank accession number NP_006696) revealed that recombinant human Gadd45γ and mutant proteins have an additional amino acid sequence (GPLGSPEF) at the N-terminus. This plasmid, containing the insert, was transformed into *Escherichia coli* strain BL21 (DE3) and overexpressed at 37°C for about 4 h by the addition of 1 mmol/L IPTG (isopropyl-β-D-thiogalactopyranoside) at OD_{600} of 0.6–0.8.

The L-SeMet human Gadd45γ protein was also expressed in *E. coli* strain BL21 (DE3). After incubation overnight in LB medium containing 100 μg/mL ampicillin, the cells were diluted with adaptive medium (20% LB medium, 80% M9 medium) and grown at 37°C to an OD_{600} of 0.6–0.8. The cells were harvested and resuspended in M9 medium, transferred into restrictive medium (5% glucose *w/v*) and then grown to an OD_{600} of 0.6–0.8 before induction. L-SeMet (Sigma) at 60 mg/L, lysine, threonine and phenylalanine at 100 mg/L, leucine, isoleucine and valine at 50 mg/L and 1 mmol/L IPTG were added and incubation continued at 16°C for about 20 h.

Several human Gadd45γ mutants, including A47R, I76E, L80E, A83R, A47R + F84R, I76E + L80E + A83R, were prepared by PCR with the Gadd45γ expression plasmid as template, using pairs of primers encoding the mutations at the sites of substitution. These mutations were constructed by use of an Easy Mutagenesis System kit (TRANS). All mutants were transformed into *Escherichia coli* strain BL21 (DE3) and over-expressed following a similar protocol of wild-type.

Protein purification

The cells were resuspended in PBS buffer (10 mmol/L Na_2HPO_4, 1.8 mmol/L KH_2PO_4, 140 mmol/L NaCl, 2.7 mmol/L KCl, pH 8.0) and immediately broken by sonication. The supernatant was applied to a glutathione Sepharose 4B (GE Healthcare, USA) column and the fusion protein was cleaved by PreScission protease at 4°C overnight. The target protein was then eluted with the buffer A (25 mmol/L Tris-HCl,150 mmol/L NaCl, pH 8.0) and loaded into a Mono Q 5/50 GL (GE Healthcare, USA) ion-exchange chromatography column run in 25 mmol/L Tris-HCl (pH 8.0), 150 mmol/L NaCl and developed with a 90 column volume gradient from 150–2000 mmol/L NaCl. The target protein was further purified by gel-filtration on a Superdex75 HR 16/60 (GE Healthcare, USA) column run in 25 mmol/L Tris-HCl (pH 8.0), 150 mmol/L NaCl. Purities of the proteins were estimated by SDS-PAGE to be greater than 95%.

Protein crystallization

The human Gadd45γ protein solution used for crystallization contained 15–40 mg/mL of protein, 25 mmol/L Tris-HCl (pH 8.0), 50 mmol/L NaCl. Crystals were obtained using the hanging-drop, vapor-diffusion technique with a reservoir solution of 0.1 mol/L Bis-Tris (pH 5.5), 0.2 mol/L NaCl, 22% (*w/v*) PEG3350 in a drop formed by mixing 1–2 μL of protein solution and 1–2 μL of reservoir solution at 291 K. The L-SeMet-labelled human Gadd45γ was purified and crystallized by the same method as for the native protein except for the addition of 5 mmol/L DTT and 0.5 mmol/L EDTA.

Data collection and processing

We collected, in total, three usable data sets. The normal diffraction data was collected to 3.0 Å resolution using X-rays of wavelength 1.000 Å. Anomalous diffraction data for the two Se-Met residues in human Gadd45 derivative was collected to 3.3 Å resolution with X-rays of wavelength 0.9803 Å at 100 K. Both data sets were collected, using a MarCCD detector on beamline 3W1A, at the Beijing Synchrotron Radiation Facility (BSRF, Beijing, China). The cryoprotectant solution contained 25% (*w/v*) PEG3350, 1 mol/L NaCl, and 0.1 mol/L Bis-Tris (pH 5.5). A third data set for native human Gadd45 was collected to 2.3 Å resolution at 100 K on beamline BL-5A of the Photon Factory (KEK, Japan) using an ADSC Q315 CCD detector. Data integrations were performed using HKL2000 (Otwinowski and Minor, 1997). Unit-cell parameters were determined to be $a = b = c = 126$ Å in space group $I2_13$ with one molecule in an asymmetric unit. Detailed data collection statistics are summarized in Table S1.

Phasing, model building and refinement

The single-wavelength anomalous diffraction (SAD) method was used for solving the phase problem with datasets 2 and 3 in Table S1. The program SHELXD correctly located the Se atom on residue Met19 in the Se-Met derivative dataset (The other Se atom on the first residue, Met1, and even all the 14 residues at the N-ternimal, including the additional 8 residues, never appear in electron density maps during the whole process of structure solving). The most probable Matthews coefficient was judged to be 2.3 $Å^3Da^{-1}$, corresponding to a solvent content of 47%, and suggesting two molecules in an assymetric unit. The initial density map from SAD, however, suggested the presence of only one molecule in one crystallographic asymmetric unit, which leads to a higher Matthews' coefficient of 4.7 $Å^3Da^{-1}$ and a higher solvent content of 73% (Fig. S1). This new value for the solvent content resulted in an experimental electron density map from SHELXE that was sufficient for manual tracing of the protein. The program COOT (Emsley and Cowtan, 2004) and REFMAC (Murshudov et al., 1997) in the CCP4 package (CCP4, 1994) were used for further model building.

The program CNS (Brünger et al., 1998) and the native dataset 1 (Table S1) were used for model refinement. The statistics on the structure refinement are summarized in Table S1.

The ribbon diagrams and surface representations were prepared using PyMol (DeLano Scientific, San Carlos, CA).

Gel filtration chromatography

After purification using glutathione Sepharose 4B (Amersham Pharmacia, USA) column and Mono Q 5/50 GL (Amersham Pharmacia) ion-exchange chromatography column, gel filtration experiments were carried out on purified human Gadd45γ and its mutants (A83R, A47R + F84R, I76R + H77R + L80R, A47R + I76E + L80E + A83R, etc.) using a Superdex™ 75 HiLoad™ 16/60 or Superdex™ 75 HiLoad™ 10/300 GL Prep Grade Column (Amersham Pharmacia) on an ÄKTA Purifier 10 system (Amersham Pharmacia) (Fig. S5A). The column was preequilibrated with buffer [25 mmol/L Tris-Cl (pH 8.0), 0.15mol/L NaCl] before injecting each sample, and absorbance data were collected at 280 nm. The column was calibrated using the low molecular weight kit from GE Healthcare (Fig. S5B).

Dynamic light scattering

Dynamic light scatting measurements were performed at 16°C using a Dynapro Titan Instrument. Wild-type Gadd45γ and mutants were dissolved into a buffer containing 20 mmol/L Tris-HCl, 150 mmol/L NaCl, pH 8.0 and were concentrated to 1 mg/mL separately (Fig. S5D).

Analytical ultracentrifugation

Sedimentation velocity (SV) and equilibrium (SE) experiments were conducted with an Optima XL-L analytical ultracentrifuge (Beckman-Coulter Instruments) (Fig. S5E and S5F). An An60Ti rotor and standard six-sector equilibrium centerpieces were used. Freshly prepared human Gadd45γ and mutants were further purified and buffer-exchanged into sedimentation buffer (150 mmol/L NaCl and 25 mmol/L Tris-HCl, pH 8.0) using a gel filtration column, and the protein concentration was determined using an Ultrospec 3300 pro UV/Visible Spectrophotometer (GE Healthcare, USA). SV analysis of the wild-type (*wt*) human Gadd45γ and two mutants (A47R + F84R, A47R + I76E + L80E + A83R) at 79 and 75, 79 μmol/L in sedimentation buffer were centrifuged at 40,000 rpm and 60,000 rpm, 20°C, respectively. Absorbance scans were carried out at a wavelength of 280 nm, and 98 scans were collected at 2 min intervals. Continuous sedimentation coefficient distributions were calculated using the *c(s)* module from the software package SEDFIT (Schuck et al., 2002). Analyses of the sedimentation velocity profiles were also performed by direct boundary modeling from solutions of the Lamm equation using the non-interaction discrete species module of SEDFIT. The analysis was performed with 95% confidence limit setting.

For sedimentation equilibrium experiments, 120 μL reference solutions and 120 μL samples (21.4, 16.5 μmol/L of Gadd45γ and 20.3, 17.2 μmol/L of Gadd45γ mutant A47R + I76E + L80E + A83R, respectively) were loaded into the cells. These proteins were equilibrated at 20°C and 18,000 rpm for 30 h, and then equilibrated again at 20°C and 20 krpm for 19 h. Each speed was maintained until there was no significant difference in $r^2/2$ versus absorbance. Once equilibrium was reached, absorption data were collected at 280 nm, using a radial step size of 3 μm, and recorded as the average of five measurements at each radial position. To determine the baseline values in the cell, the rotor speed was increased to 42,000 rpm for 5 h at the end of each data collection, and the absorbance of the depleted meniscus was measured. The solution densities and V-bar (partial specific volumes) of different samples were calculated with the program SEDNTERP (Laue et al., 1991). The monomer molecular weights and theoretical extinction coefficient were calculated from the amino acid sequences with the program SEDNTERP. Dissociation constants (K_d) were determined by fitting a monomer-dimer equilibrium model using the Origin-based data analysis software (Origin 6.0, Beckman) for the Beckman XL-L (Beckman Instruments, Beckman Coulter, Fullerton, CA). Data from different loading concentrations were combined for global fitting.

Protein lysate preparation

For whole cell protein extraction, Hela cells were harvested, washed with phosphate buffered saline (PBS) and lysed in lysis buffer [1×PBS, 1% Nonidet P-40, 2 mg/mL aprotinin, 2 mg/mL leupeptin and 50 mg/mL phenylmethylsulfonyl fluoride (PMSF)]. Cell lysates were kept on ice for 40 min and centrifuged at 14,000 g at 4°C for 20 min. Then supernatants were collected as total protein lysates.

GST pull-down assay

Glutathione-agarose bead-conjugated GST fusion proteins were incubated with 2 mg protein lysates at 4°C overnight, centrifuged and 20 μL supernatant was reserved to analyze actin as control. After gently washing 3–5 times with lysis buffer, glutathione-agarose beads were boiled in SDS-PAGE loading buffer, separated by 12% sodium dodecyl sulfate-polyacrylamide gel electrophoresis (SDS-PAGE) and transferred to nitrocellulose membranes. Membranes were incubated with primary antibodies and anti-mouse secondary antibodies

conjugated to horseradish peroxidase for enhanced chemiluminescence detection of the signals.

Colony formation assay

Human wild-type Gadd45γ and mutants were subcloned into *Xho*I/*Xba*I sites of the mammalian expression vector pcDNA3.1(+) (Invitrogen). EC9706 and HeLa cells were transfected with lipofectamine (Invitrogen) according to the manufacturer's protocol. 24 h after transfection, cells were replated and selected for 2–3 weeks with G418. Surviving colonies ($\geqslant$ 50 cells per colony) were counted after staining with 0.5% crystal violet.

Cell cycle analysis

HeLa cells were transfected with the indicated pcDNA3.1(+) vectors using Lipofectamine. Cells were harvested 48 h later, washed with phosphate-buffered saline and fixed with ice-cold 70% ethanol at −20°C overnight. Samples were washed with phosphate-buffered saline and stained with propidium iodide (Sigma) containing RNase A (Sigma) for 30 min at 37°C. Distribution in different phases of cell cycle was determined using flow cytometry.

Apoptosis assay

Full-length human wild-type Gadd45γ and indicated mutant forms were subcloned into the *Eco*RI/*Xho*I sites of the mammalian expression vector pCS2 + MT with the Myc tag. HeLa cells, following transfection for 24 h with indicated pCS2 + MT vectors, were exposed to both low and high doses of UV irradiation (8 J/m^2 and 40 J/m^2, respectively), after which cells were cultured for 24 h. Cells were fixed and permeabilized by immersion in cold methanol (−20°C) for 15 min. After washing three times with PBS, cells were incubated with anti-Myc antibody (1:250) for 2 h at room temperature, followed by TRITC-conjugated secondary antibody incubation (1:150). Cells were stained with DAPI (0.1 μg/mL) and examined under a fluorescence microscope.

Statistical analysis

Most experiments were performed and repeated at least three times. Data were represented as mean ± SD. Statistical analysis was performed by one-way ANOVA and unpaired two-tailed *t* test, using SPSS16.0 and Microsoft Excel. $p < 0.05$ was considered significant.

ACKNOWLEDGEMENTS

We thank Yingfang Liu, Fei Sun, Zhiyong Lou, Zhushan Zhang and Xuejun C. Zhang for valuable discussion; beamline staff at BSRF and KEK for their help with data collection; and staff of Structural Biology Core Facility in IBP for their technical assistance. This work was supported by the National Basic Research Program (973 Program) (Nos. 2006CB806503, 2007CB914301 and 2007CB914304), the National Programs for High Technology Research and Development Program (863 Program) (No. 2006AA02A322) and the National Major Project (Grant No. 2009ZX10004-304). The atomic coordinates and structure factors have been deposited in the Protein Data Bank with the accession number 3FFM.

Supplementary material is available in the online version of this article at http://dx.doi.org/10.1007/s13238-011-1090-6 and is accessible for authorized users.

ABBREVIATIONS

AUC, a nalytical ultracentrifugation; GST, glutathione S transferase; IPTG, isopropyl-β-D-thiogalactopyranoside; MW, molecular weights; PBS, phosphate buffered saline; PCNA, proliferating cell nuclear antigen; PDB, Protein Data Bank; PI, propidium iodide; PMSF, phenylmethylsulfonyl fluoride; SAD, single-wavelength anomalous diffraction; SE, sedimentation equilibrium; SV, sedimentation velocity

REFERENCES

Azam, N., Vairapandi, M., Zhang, W., Hoffman, B., and Liebermann, D.A. (2001). Interaction of CR6 (GADD45gamma) with proliferating cell nuclear antigen impedes negative growth control. J Biol Chem 276, 2766–2774.

Barreto, G., Schäfer, A., Marhold, J., Stach, D., Swaminathan, S.K., Handa, V., Döderlein, G., Maltry, N., Wu, W., Lyko, F., *et al.* (2007). Gadd45a promotes epigenetic gene activation by repair-mediated DNA demethylation. Nature 445, 671–675.

Brünger, A.T., Adams, P.D., Clore, G.M., DeLano, W.L., Gros, P., Grosse-Kunstleve, R.W., Jiang, J.S., Kuszewski, J., Nilges, M., Pannu, N.S., *et al.* (1998). Crystallography & NMR system: A new software suite for macromolecular structure determination. Acta Crystallogr D Biol Crystallogr 54, 905–921.

Bulavin, D.V., Kovalsky, O., Hollander, M.C., and Fornace, A.J. Jr. (2003). Loss of oncogenic H-ras-induced cell cycle arrest and p38 mitogen-activated protein kinase activation by disruption of Gadd45a. Mol Cell Biol 23, 3859–3871.

Carrier, F., Georgel, P.T., Pourquier, P., Blake, M., Kontny, H.U., Antinore, M.J., Gariboldi, M., Myers, T.G., Weinstein, J.N., Pommier, Y., *et al.* (1999). Gadd45, a p53-responsive stress protein, modifies DNA accessibility on damaged chromatin. Mol Cell Biol 19, 1673–1685.

Chung, H.K., Yi, Y.W., Jung, N.C., Kim, D., Suh, J.M., Kim, H., Park, K. C., Song, J.H., Kim, D.W., Hwang, E.S., *et al.* (2003). CR6-interacting factor 1 interacts with Gadd45 family proteins and modulates the cell cycle. J Biol Chem 278, 28079–28088.

Emsley, P., and Cowtan, K. (2004). Coot: model-building tools for molecular graphics. Acta Crystallogr D Biol Crystallogr 60, 2126–2132.

Fan, W., Richter, G., Cereseto, A., Beadling, C., and Smith, K.A. (1999). Cytokine response gene 6 induces p21 and regulates both cell growth and arrest. Oncogene 18, 6573–6582.

Furukawa-Hibi, Y., Yoshida-Araki, K., Ohta, T., Ikeda, K., and Motoyama, N. (2002). FOXO forkhead transcription factors induce G(2)-M checkpoint in response to oxidative stress. J Biol Chem 277, 26729–26732.

Gao, H., Jin, S., Song, Y., Fu, M., Wang, M., Liu, Z., Wu, M., and Zhan, Q. (2005). B23 regulates GADD45a nuclear translocation and contributes to GADD45a-induced cell cycle G2-M arrest. J Biol Chem 280, 10988–10996.

Harkin, D.P., Bean, J.M., Miklos, D., Song, Y.H., Truong, V.B., Englert, C., Christians, F.C., Ellisen, L.W., Maheswaran, S., Oliner, J.D., *et al.* (1999). Induction of GADD45 and JNK/SAPK-dependent

apoptosis following inducible expression of BRCA1. Cell 97, 575–586.

Jin, S., Antinore, M.J., Lung, F.D., Dong, X., Zhao, H., Fan, F., Colchagie, A.B., Blanck, P., Roller, P.P., Fornace, A.J. Jr, *et al.* (2000). The GADD45 inhibition of Cdc2 kinase correlates with GADD45-mediated growth suppression. J Biol Chem 275, 16602–16608.

Jin, S., Tong, T., Fan, W., Fan, F., Antinore, M.J., Zhu, X., Mazzacurati, L., Li, X., Petrik, K.L., Rajasekaran, B., *et al.* (2002). GADD45-induced cell cycle G2-M arrest associates with altered subcellular distribution of cyclin B1 and is independent of p38 kinase activity. Oncogene 21, 8696–8704.

Jung, N., Yi, Y.W., Kim, D., Shong, M., Hong, S.S., Lee, H.S., and Bae, I. (2000). Regulation of Gadd45gamma expression by C/EBP. Eur J Biochem 267, 6180–6187.

Kastan, M.B., Zhan, Q., el-Deiry, W.S., Carrier, F., Jacks, T., Walsh, W.V., Plunkett, B.S., Vogelstein, B., and Fornace, A.J. Jr. (1992). A mammalian cell cycle checkpoint pathway utilizing p53 and GADD45 is defective in ataxia-telangiectasia. Cell 71, 587–597.

Kearsey, J.M., Coates, P.J., Prescott, A.R., Warbrick, E., and Hall, P. A. (1995). Gadd45 is a nuclear cell cycle regulated protein which interacts with p21Cip1. Oncogene 11, 1675–1683.

Kovalsky, O., Lung, F.D., Roller, P.P., and Fornace, A.J. Jr. (2001). Oligomerization of human Gadd45a protein. J Biol Chem 276, 39330–39339.

Kraulis, P.J. (1991). MOLSCRIPT: a program to produce both detailed and schematic plots of protein structures. J Appl Cryst 24, 946–950.

Laue, T., Shaw, B.D., Ridgeway, T.M., and Pelletier, S.L. (1991). Computer-aided Interpretation of Analytical Sedimentation Data For Proteins. In: Analytical Ultracentrifugation in Biochemistry and Polymer Science. Harding S.E., Rowe A.J., and Horton J.C., eds. Cambridge, UK: Royal Soc Chem. 90–125.

Lefort, K., Rouault, J.P., Tondereau, L., Magaud, J.P., and Doré, J.F. (2001). The specific activation of gadd45 following UVB radiation requires the POU family gene product N-oct3 in human melanoma cells. Oncogene 20, 7375–7385.

Liebermann, D.A., and Hoffman, B. (2007). Gadd45 in the response of hematopoietic cells to genotoxic stress. Blood Cells Mol Dis 39, 329–335.

Mak, S.K., and Kültz, D. (2004). Gadd45 proteins induce G2/M arrest and modulate apoptosis in kidney cells exposed to hyperosmotic stress. J Biol Chem 279, 39075–39084.

Merritt, E.A., and Bacon, D.J. (1997). Raster3D: photorealistic molecular graphics. Methods Enzymol 277, 505–524.

Murshudov, G.N., Vagin, A.A., and Dodson, E.J. (1997). Refinement of macromolecular structures by the maximum-likelihood method. Acta Crystallogr D Biol Crystallogr 53, 240–255.

Nakayama, K., Hara, T., Hibi, M., Hirano, T., and Miyajima, A. (1999). A novel oncostatin M-inducible gene OIG37 forms a gene family with MyD118 and GADD45 and negatively regulates cell growth. J Biol Chem 274, 24766–24772.

Otwinowski, Z., and Minor, W. (1997). Processing of X-ray Diffraction Data Collected in Oscillation Mode. In: Macromolecular Crystallography. Carter C.W. Jr., and Sweet R.M., eds. New York: Academic. 307–326.

Papa, S., Zazzeroni, F., Bubici, C., Jayawardena, S., Alvarez, K., Matsuda, S., Nguyen, D.U., Pham, C.G., Nelsbach, A.H., Melis, T., *et al.* (2004). Gadd45 beta mediates the NF-kappa B suppression of JNK signalling by targeting MKK7/JNKK2. Nat Cell Biol 6, 146–153.

Schrag, J.D., Jiralerspong, S., Banville, M., Jaramillo, M.L., and O'Connor-McCourt, M.D. (2008). The crystal structure and dimerization interface of GADD45gamma. Proc Natl Acad Sci U S A 105, 6566–6571.

Schuck, P., Perugini, M.A., Gonzales, N.R., Howlett, G.J., and Schubert, D. (2002). Size-distribution analysis of proteins by analytical ultracentrifugation: strategies and application to model systems. Biophys J 82, 1096–1111.

Shao, S., Wang, Y., Jin, S., Song, Y., Wang, X., Fan, W., Zhao, Z., Fu, M., Tong, T., Dong, L., *et al.* (2006). Gadd45a interacts with aurora-A and inhibits its kinase activity. J Biol Chem 281, 28943–28950.

Smith, G.B., and Mocarski, E.S. (2005). Contribution of GADD45 family members to cell death suppression by cellular Bcl-xL and cytomegalovirus vMIA. J Virol 79, 14923–14932.

Smith, M.L., Chen, I.T., Zhan, Q., Bae, I., Chen, C.Y., Gilmer, T.M., Kastan, M.B., O'Connor, P.M., and Fornace, A.J. Jr. (1994). Interaction of the p53-regulated protein Gadd45 with proliferating cell nuclear antigen. Science 266, 1376–1380.

Smith, M.L., Ford, J.M., Hollander, M.C., Bortnick, R.A., Amundson, S.A., Seo, Y.R., Deng, C.X., Hanawalt, P.C., and Fornace, A.J. Jr. (2000). p53-mediated DNA repair responses to UV radiation: studies of mouse cells lacking p53, p21, and/or gadd45 genes. Mol Cell Biol 20, 3705–3714.

Sun, L., Gong, R., Wan, B., Huang, X., Wu, C., Zhang, X., Zhao, S., and Yu, L. (2003). GADD45gamma, down-regulated in 65% hepatocellular carcinoma (HCC) from 23 chinese patients, inhibits cell growth and induces cell cycle G2/M arrest for hepatoma Hep-G2 cell lines. Mol Biol Rep 30, 249–253.

Takekawa, M., and Saito, H. (1998). A family of stress-inducible GADD45-like proteins mediate activation of the stress-responsive MTK1/MEKK4 MAPKKK. Cell 95, 521–530.

Thyss, R., Virolle, V., Imbert, V., Peyron, J.F., Aberdam, D., and Virolle, T. (2005). NF-kappaB/Egr-1/Gadd45 are sequentially activated upon UVB irradiation to mediate epidermal cell death. EMBO J 24, 128–137.

Tornatore, L., Marasco, D., Dathan, N., Vitale, R.M., Benedetti, E., Papa, S., Franzoso, G., Ruvo, M., and Monti, S.M. (2008). Gadd45 beta forms a homodimeric complex that binds tightly to MKK7. J Mol Biol 378, 97–111.

Vairapandi, M., Azam, N., Balliet, A.G., Hoffman, B., and Liebermann, D.A. (2000). Characterization of MyD118, Gadd45, and proliferating cell nuclear antigen (PCNA) interacting domains. PCNA impedes MyD118 AND Gadd45-mediated negative growth control. J Biol Chem 275, 16810–16819.

Vairapandi, M., Balliet, A.G., Fornace, A.J. Jr, Hoffman, B., and Liebermann, D.A. (1996). The differentiation primary response gene MyD118, related to GADD45, encodes for a nuclear protein which interacts with PCNA and p21WAF1/CIP1. Oncogene 12, 2579–2594.

Vairapandi, M., Balliet, A.G., Hoffman, B., and Liebermann, D.A. (2002). GADD45b and GADD45g are cdc2/cyclinB1 kinase inhibitors with a role in S and G2/M cell cycle checkpoints induced by genotoxic stress. J Cell Physiol 192, 327–338.

Wang, X.W., Zhan, Q., Coursen, J.D., Khan, M.A., Kontny, H.U., Yu, L., Hollander, M.C., O'Connor, P.M., Fornace, A.J. Jr, and Harris, C.C. (1999). GADD45 induction of a G2/M cell cycle checkpoint. Proc Natl Acad Sci U S A 96, 3706–3711.

Zhan, Q., Antinore, M.J., Wang, X.W., Carrier, F., Smith, M.L., Harris, C.C., and Fornace, A.J. Jr. (1999). Association with Cdc2 and inhibition of Cdc2/Cyclin B1 kinase activity by the p53-regulated protein Gadd45. Oncogene 18, 2892–2900.

Zhao, H., Jin, S., Antinore, M.J., Lung, F.D., Fan, F., Blanck, P., Roller, P., Fornace, A.J. Jr, and Zhan, Q. (2000). The central region of Gadd45 is required for its interaction with p21/WAF1. Exp Cell Res 258, 92–100.

